

Dynein and dynactin deficiencies affect the formation and function of the Spitzenkörper and distort hyphal morphogenesis of *Neurospora crassa*

Meritxell Riquelme,¹ Gerhard Gierz² and Salomon Bartnicki-García¹

Author for correspondence: Salomon Bartnicki-García. Tel: +1 909 787 4135. Fax: +1 909 787 4294. e-mail: bart@ucrac1.ucr.edu

Department of Plant Pathology¹ and Department of Mathematics², University of California, Riverside, CA 92521-0122, USA

The impact of mutations affecting microtubule-associated motor proteins on the morphology and cytology of hyphae of *Neurospora crassa* was studied. Two *ropy* mutants, *ro-1* and *ro-3*, deficient in dynein and dynactin, respectively, were examined by video-enhanced phase-contrast microscopy and image analysis. In contrast to the regular, *hyphoid* morphology of wild-type hyphae, the hyphae of the *ropy* mutants exhibited a great variety of distorted, non-hyphoid morphologies. The *ropy* hyphae were slow-growing and manifested frequent loss of growth directionality. Cytoplasmic appearance, including organelle distribution and movement, were ostensibly different in the *ropy* hyphae. The Spitzenkörper (Spk) of wild-type hyphae was readily seen by phase-contrast optics; the Spk of both *ro-1* and *ro-3* was less prominent and sometimes undetectable. Only the fast-growing *ropy* hyphae displayed a Spk, and it was smaller and less phase-dark than the wild-type Spk. Growth rate in both wild-type and *ropy* mutants was directly correlated with the size of the Spk. Spk efficiency, measured in terms of cell area generated per Spk travelled distance, was lower in *ropy* mutants. Another salient difference between *ropy* mutants and wild-type hyphae was in Spk trajectory. Whereas the Spk of wild-type hyphae maintained a trajectory close to the cell growth axis, the Spk of *ropy* hyphae moved much more erratically. Sustained departures in the trajectory of the *ropy* Spk produced corresponding distortions in hyphal morphology. A causal correlation between Spk trajectory and cell shape was tested with the Fungus Simulator program. The characteristic morphologies of wild-type or *ropy* hyphae were reproduced by the Fungus Simulator, whose vesicle supply centre (VSC) was programmed to follow the corresponding Spk trajectories. This is evidence that the Spk controls hyphal morphology by operating as a VSC. These findings on dynein or dynactin deficiency support the notion that the microtubular cytoskeleton plays a major role in the formation and positioning of the Spk, with dramatic consequences on hyphal growth and morphogenesis.

Keywords: *ropy* mutants, Spitzenkörper, *Neurospora crassa*

INTRODUCTION

This study is part of a project to elucidate the role of the Spitzenkörper (Spk) in hyphal growth and morphogenesis of higher fungi. In the present work, we used video-enhanced phase-contrast microscopy and image

analysis to examine the behaviour of morphological mutants of *Neurospora crassa* affected in genes encoding microtubule-associated motor proteins.

The Spk is a dynamic body whose structure varies widely among fungi; it usually consists of an outer vesicle cloud and an inner core (López-Franco & Bracker, 1996). In addition to vesicles (Girbardt, 1969; Grove & Bracker, 1970), other components have

.....
Abbreviations: Spk, Spitzenkörper; VSC, vesicle supply centre.

been detected in the Spk, including amorphous or granular material of undefined nature in the core region as well as components of the cytoskeleton and ribosomes (McClure *et al.*, 1968; Turian, 1978; Bourett & Howard, 1991; Roberson & Vargas, 1994; López-Franco & Bracker, 1996). The morphology of the fungal cells is determined by the way the cell wall is assembled (Bartnicki-García, 1968, 1973). In hyphae, cell wall growth occurs mainly at the tip by polarized secretion of enzymes and cell wall precursors (Bartnicki-García & Lippman, 1969; Trinci, 1978; Harold, 1990). There is a sizeable body of evidence that the Spk plays a central role in apical growth and morphogenesis (Girbardt, 1957; López-Franco & Bracker, 1996; Reynaga-Peña & Bartnicki-García, 1997). According to the vesicle supply centre (VSC) model for fungal morphogenesis (Bartnicki-García *et al.*, 1989), the Spk functions as a vesicle distribution centre. Vesicles generated in distal parts of the hypha congregate in the Spk and from there migrate to the cell surface. The linear displacement of the Spk creates a sharp gradient of exocytosis responsible for hyphal morphogenesis.

There is mounting evidence that the position of the Spk governs the growth direction of a hypha (Girbardt, 1957; Bracker *et al.*, 1997; Riquelme *et al.*, 1998). Our previous work with microtubule inhibitors implicated the microtubular cytoskeleton in the positioning and movement of the Spk in hyphae of *N. crassa* (Riquelme *et al.*, 1998), but its exact role in apical growth has yet to be elucidated. It has long been proposed that cytoplasmic microtubules participate in the transport of secretory vesicles to the hyphal apex (Howard & Aist, 1977, 1980; Howard, 1981; Gooday, 1983; Gow, 1989; Hasek & Bartnicki-García, 1994; McKerracher & Heath, 1987; Heath, 1994). The discovery of microtubule-associated motor proteins (Hirokawa, 1982; Paschal *et al.*, 1987) has helped us understand how organelles move inside the cell. Cytoplasmic dyneins and members of the kinesin superfamily are the main motor enzymes involved in vesicle translocation along microtubules (Haimo & Thaler, 1994; Hirokawa, 1998). There is now growing evidence that both kinesins and cytoplasmic dyneins are involved in the traffic of secretory vesicles in fungal hyphae (Seiler *et al.*, 1997; Wu *et al.*, 1998; Inoue *et al.*, 1998). Cytoplasmic dyneins are multisubunit enzymes involved in transport of membranous organelles towards the minus end of microtubules (Paschal *et al.*, 1987; Schroer & Sheetz, 1991; Hirokawa, 1998). Kinesins are motor proteins involved in membrane transport towards the plus end of the microtubules (Vale *et al.*, 1985; Hirokawa, 1982; Steinberg & Schliwa, 1996).

To examine the relationship among the Spk, the microtubular cytoskeleton and hyphal morphogenesis, we chose two *ropy* mutants of *N. crassa*, *ro-1* and *ro-3*. Both belong to the group of true colonial morphological mutants (Garnjobst & Tatum, 1967; Vierula, 1996) and have been characterized at the molecular level. Mutant *ro-1* is deficient in one of the heavy chains of cytoplasmic dynein (Plamann *et al.*, 1994). Mutant *ro-3* is deficient in

p150^{Glued}, the largest subunit of the dynactin (dynein activator) complex (Plamann *et al.*, 1994; Tinsley *et al.*, 1996). Dynactin is a multisubunit complex required for cytoplasmic dynein to efficiently transport vesicles along microtubules *in vitro* (Gill *et al.*, 1991; Schroer & Sheetz, 1991).

Most studies on *ropy* mutants have primarily focused on the aberrant distribution of nuclei in *ro-1* and *ro-3* hyphae and on the molecular characterization of those loci (Plamann *et al.*, 1994; Bruno *et al.*, 1996; Tinsley *et al.*, 1996). Since hyphal and, ultimately, colony morphology are largely established at the hyphal apex, we have focused this study on the impact of the *ropy* mutations on apical events, where most of the growth process is concentrated.

METHODS

Strains and media. *N. crassa* wild-type (FGSC 988) and *ropy* strains (FGSC 4351 and 43 for *ro-1* and *ro-3* respectively) were obtained from the Fungal Genetics Stock Center. The strains were grown and maintained in 8.5 cm plastic Petri dishes (sold as 100 × 15 mm, Fischer Scientific) containing 20 ml Vogel's Complete Medium (VCM) agar (Vogel, 1956) with 1.5% (w/v) sucrose as the carbon source. Cultures were grown at 21 °C.

Video microscopy. Growing hyphae were observed with an Olympus Vanox-S microscope. For low-magnification images, the fungus was grown in 8.5 cm plastic Petri dishes on a thin layer (10 ml) of VCM agar at 21 °C and observed with bright-field optics (10× objective and 10× WF eyepiece). For high-resolution work, the fungus was grown on a modified slide culture chamber (López-Franco, 1992; Riquelme *et al.*, 1998) and observed with a phase-contrast 100× oil-immersion objective (n.a. 1.25) and a 25× WF eyepiece (American Optical).

Video images were produced with a Hamamatsu C2400-07 high-resolution camera (Hamamatsu Photonic Systems), enhanced with an Argus-10 image processor (a real-time digital contrast and low light enhancement system), and displayed on a black and white, 12-inch, high-resolution monitor (Sony; model PVM-122). Sequences were videotaped in real time with an S-VHS recorder (JVC model BR-S822U).

Growth rate and cell parameters measurements. Videotaped sequences were played on a variable-tracking player (JVC model BR-S525U) and observed on a Sony Trinitron model monitor. Individual images were captured from the videotaped sequences in 8-bit greyscale with an Imascan/Chroma frame grabber (Imagraph). With Image Pro Plus Software for Windows (Media Cybernetics), we traced the cell profiles of the images captured by video microscopy. *xy* coordinate values were automatically collected into a text file with a Windows application program interfaced with the Argus-10 analyser (Bartnicki *et al.*, 1994). The text files were then imported into Microsoft Excel spreadsheets and analysed.

Growth rate was measured in terms of cell area increase. Typically, measurements were made during growth periods of 1–4 min depending on growth rate and availability of well-defined profiles. For convenience and accuracy, only images within the same field of view were compared. The area delimited by the cell profiles was computed by using Green's formula (Marsden *et al.*, 1993). Spk diameter was measured

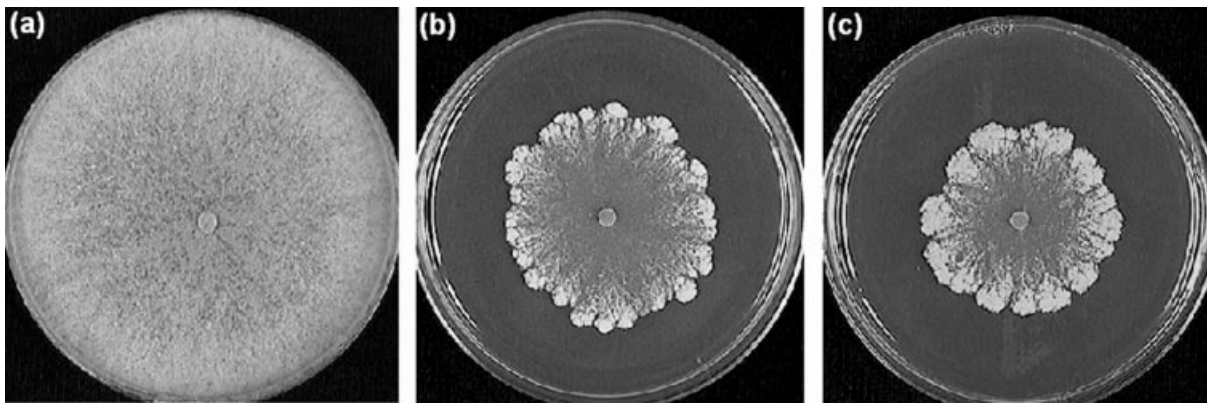


Fig. 1. Colonies of *N. crassa* wild-type (a), *ro-1* (b) and *ro-3* (c) grown on VCM (20 ml) for 24 h at 28 °C.

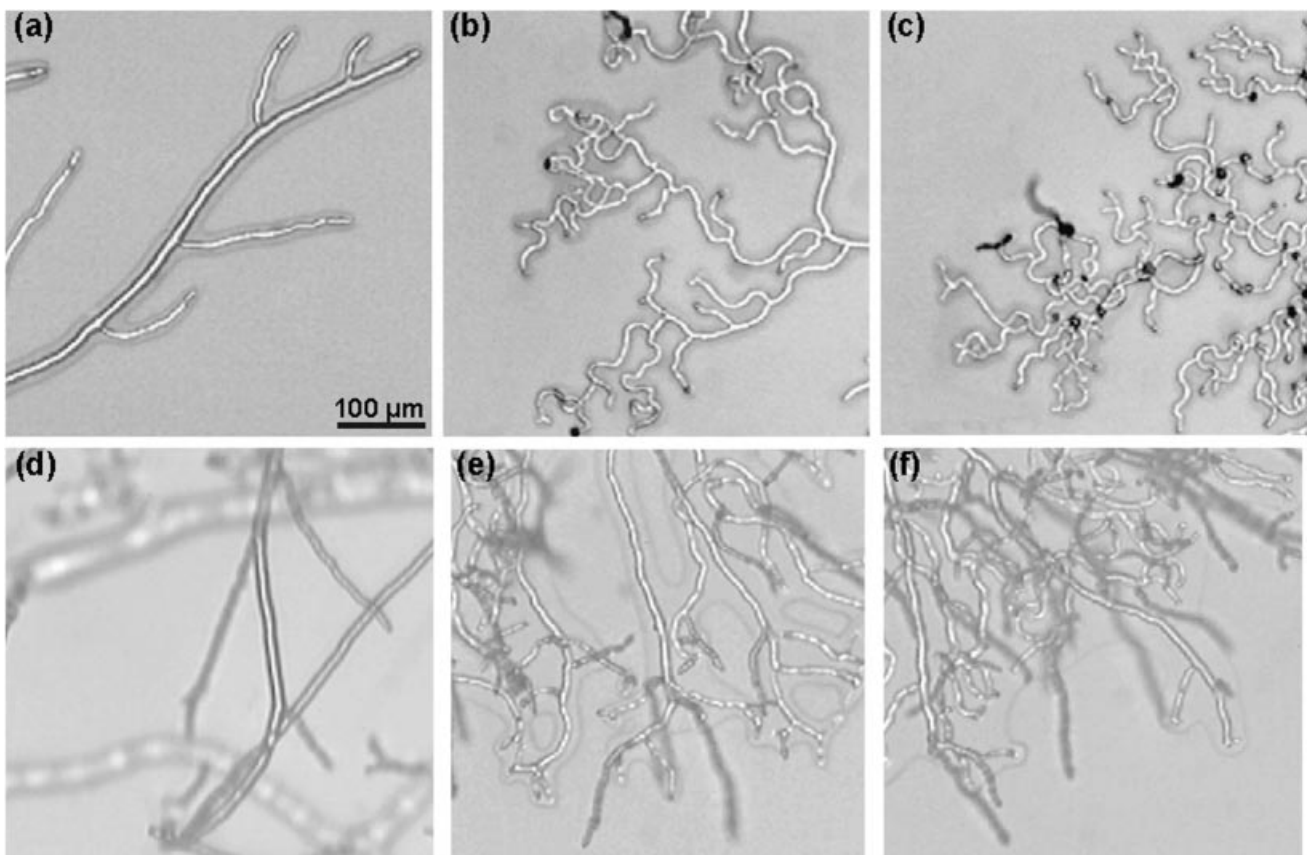


Fig. 2. Bright-field micrographs of hyphae of *N. crassa* wild-type (a, d), *ro-1* (b, e) and *ro-3* (c, f). Top row after 14 h growth; bottom row after 24 h growth.

directly on the monitor screen with the line command of the measure option in the Argus-10 menu.

Spk trajectory analysis. The centre of the Spk was mapped at 2 s intervals from the videotaped sequences. To quantitate the erratic behaviour of the advancing Spk, we calculated a steadiness index (S), namely the ratio of the minimal distance between the initial and final position of the Spk in a given videotaped sequence over the total distance travelled by the

Spk. A steadiness index of 1 would correspond to a perfectly straight path. The smaller the steadiness index the less steady the trajectory of the Spk.

Computer simulation. From videotaped sequences of hyphae of wild-type and *ropy* mutants, we mapped the Spk position (every 2 s) and traced the cell profiles at various intervals. These data were fed to the Fungus Simulator [a Windows program for fungal morphogenesis (Bartnicki *et al.*, 1994)

available through the Internet (<http://boyce3427.ucr.edu>). The Fungus Simulator generates hyphal shapes by a process that mimics a vesicle-based mechanism for cell wall growth.

RESULTS

Colony and hyphal morphology

On agar plates, the two *ropy* mutants formed colonies that were drastically different from the wild-type. Radial growth was restricted and the aerial mycelium showed the characteristic *ropy* phenotype (Fig. 1).

Under the microscope, the *ropy* mutants showed remarkable differences in hyphal morphology compared to the wild-type (Fig. 2). In a young colony (8–14 h), the morphology of *ropy* hyphae was highly irregular, with extensive curling – an indication of a major loss in growth directionality (Fig. 2b, c). In contrast, the hyphae of the wild-type were more regular, and despite some minor meandering they exhibited long stretches of mostly straight growth (Fig. 2a). In older colonies (> 14 h), the morphology of hyphae growing on the agar surface remained the same but the *ropy* mutants produced large cottony tufts of aerial hyphae at the periphery of the colony. This aerial mycelium consisted

of some very long and straight primary hyphae (Fig. 2e, f) with numerous short curly branches. In the wild-type, mycelium spread faster on the agar surface, producing a flatter and more uniform mat of aerial hyphae. Both surface and aerial hyphae grew rather straight (Fig. 2d).

At high magnification, most wild-type hyphae (Fig. 3a, b) showed a regular apical profile that approximated the ideal shape defined by the hyphoid equation $y = x \cot(xV/N)$. There were also some slow-growing wild-type hyphae that deviated appreciably from this hyphoid morphology (Fig. 3c). In contrast, the hyphae of the *ropy* mutants exhibited a great variety of distorted, non-hyphoid morphologies: some apices were blunt, others more pointed; often, the hyphal profile was highly irregular with conspicuous swellings (Fig. 3d–i).

Cytoplasmic appearance

As visualized by phase-contrast microscopy (Fig. 3), there were major differences in cytoplasmic appearance between hyphae of the *ropy* mutants and wild-type. In the apex of wild-type hyphae, the dominant structure was a large phase-dark Spk (Fig. 3a, b) that corresponds to the organizational pattern 8 described by López-

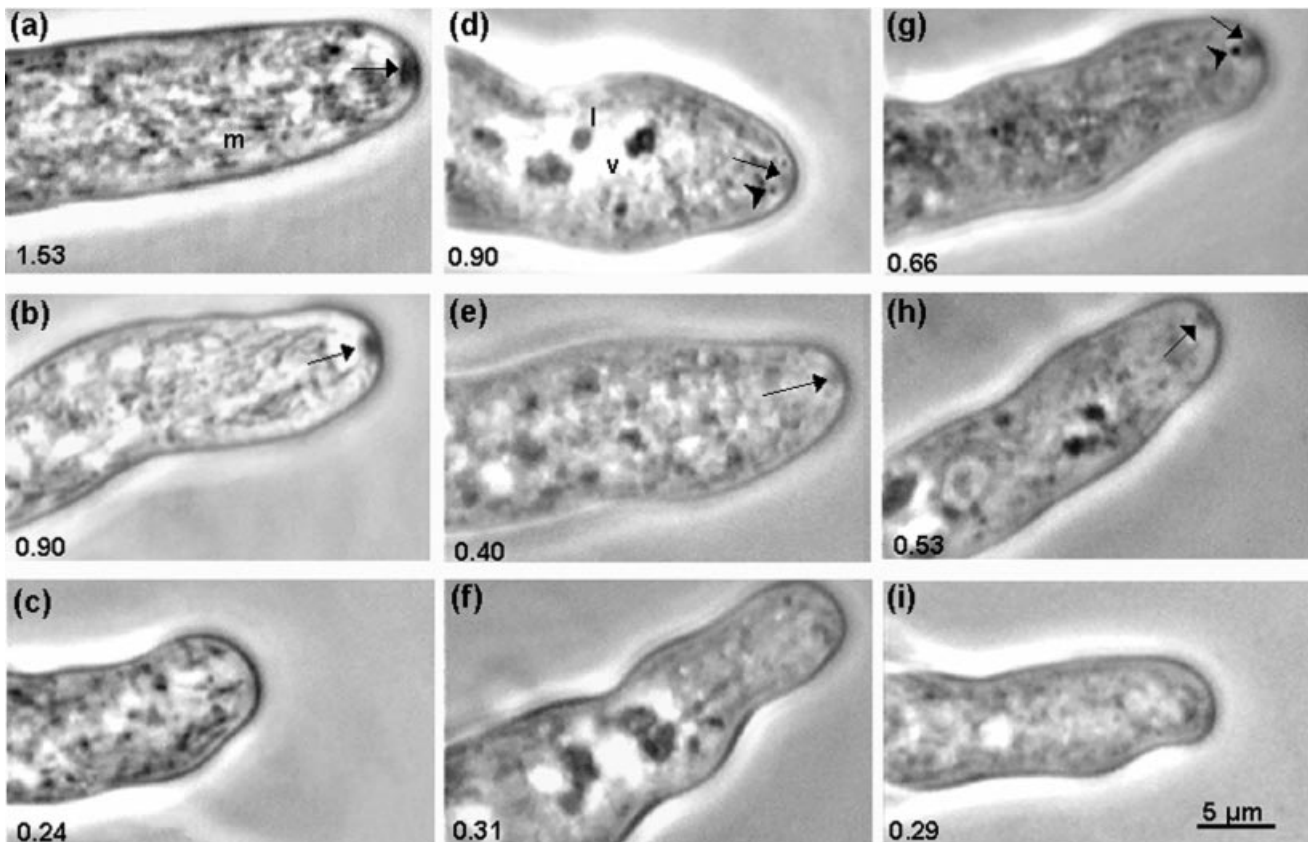


Fig. 3. Variation in hyphal tip morphology in wild-type and *ropy* mutants of *N. crassa*. Phase-contrast micrographs of wild-type (a–c), *ro-1* (d–f) and *ro-3* (g–i) hyphae. Numbers indicate growth rate in $\mu\text{m}^2 \text{s}^{-1}$. Arrows, Spk; m, mitochondria; v, vacuoles; l, lipid bodies. Arrowheads (in d and g) point at a phase-dark globular body.

Table 1. Cell parameters of *N. crassa* wild-type, *ro-1* and *ro-3*Data are mean values \pm SD.

Strain*	No. of hyphae analysed	Growth rate ($\mu\text{m}^2 \text{s}^{-1}$)	Hyphal diameter (μm)†	Spk diameter (μm)‡
Wild-type	4	3.47 \pm 0.63	10.67 \pm 1.03	1.85 \pm 0.14
	4	1.42 \pm 0.20	9.82 \pm 0.60	1.35 \pm 0.15
	4	0.84 \pm 0.07	8.28 \pm 0.88	1.32 \pm 0.30
	4	0.61 \pm 0.16	7.36 \pm 1.97	1.05 \pm 0.32
	3	0.28 \pm 0.04	8.92 \pm 1.98	§
<i>ro-1</i>	5	1.38 \pm 0.48	8.96 \pm 1.54	1.02 \pm 0.31
	5	0.77 \pm 0.06	7.19 \pm 0.48	0.82 \pm 0.23
	5	0.50 \pm 0.07	8.29 \pm 2.36	0.93 \pm 0.28
	4	0.24 \pm 0.10	6.60 \pm 0.82	0.67 \pm 0.36
	3	0.09 \pm 0.02	6.97 \pm 2.70	§
<i>ro-3</i>	5	0.83 \pm 0.22	8.02 \pm 0.89	0.81 \pm 0.12
	4	0.57 \pm 0.03	7.85 \pm 0.46	0.96 \pm 0.12
	4	0.41 \pm 0.08	7.13 \pm 1.24	0.84 \pm 0.05
	4	0.29 \pm 0.04	7.05 \pm 1.44	0.72 \pm 0.04
	2	0.15 \pm 0.03	5.69 \pm 0.12	§

* For each strain, the values for individual hyphae (Fig. 4) were organized in subgroups in descending order of growth rate.

† Hyphal diameter was calculated by dividing the hyphal area by the length of the hypha.

‡ During each growth sequence, Spk diameter was measured when it was most clearly defined.

§ No Spk was visible.

Franco & Bracker (1996). In the *ropy* mutants, the Spk was smaller and less phase-dark (Fig. 3d, e, g, h). In the subapex, there were also marked differences between wild-type and *ropy*. In general, organelle distribution was more uniform in the wild-type. A remarkable difference was in the appearance of mitochondria. In the wild-type strain, these long, phase-dark organelles were the dominant structure of the cytoplasm. In the *ropy*

mutants, the mitochondria were round and less conspicuous, giving the cytoplasm a more finely granular appearance, particularly in slower-growing hyphae.

Another common difference was in vacuolation. The cytoplasm of both *ropy* mutants was more vacuolated than in wild-type. In *ropy* hyphae, large, phase-light and phase-dark structures of irregular shape (probably vacuoles and lipid bodies) accumulated at a shorter distance (as close as 10–15 μm) from the tip. Occasionally, one or more small phase-dark globular bodies were seen immediately behind the Spk (Fig. 3d, g; arrowheads). These bodies moved continuously within the area surrounding the Spk but appeared to be physically attached to the Spk by thin filaments and remained behind the Spk for the entire observation period. These granules were usually more conspicuous in the *ropy* mutants but were some times seen in tips of wild-type hyphae. Similar structures have been seen in other fungi (López-Franco & Bracker, 1996) but their function remains unknown.

There was a pronounced difference in overall movement of cytoplasmic structures between wild-type and *ropy* mutants. To judge differences in organelle movement, the videotaped growth sequences were examined in real time and at three times the original speed. The cytoplasm in the hyphae of *ropy* mutants was ostensibly less dynamic than that in wild-type hyphae. In the latter, cytoplasmic organelles were in constant motion over the entire length of the subapical area observed (at least 20–25 μm from the apex). In *ropy* hyphae, motion was less active and was usually restricted to the proximal subapex (5–15 μm from the apex); beyond that, the cytoplasm became static and extensively vacuolated (Fig. 3; see also video in <http://boyce3427.ucr.edu/cytoskel.htm>). In both *ropy* mutants, the movement of cytoplasmic structures appeared less organized than that in wild-type hyphae. In growing wild-type hyphae, the mitochondria moved continuously in a back and forth fashion roughly parallel to the longitudinal axis of growth. In the *ropy* mutants, mitochondria did not move preferentially along the longitudinal axis but in a more erratic manner.

Table 2. Cell parameters of *N. crassa* wild-type, *ro-1* and *ro-3*

Values for each strain are the mean of all cells analysed in Table 1. Means within each column followed by the same letter are not significantly different ($P = 0.05$) according to Student's *t*-test analysis.

Strain	No. of hyphae analysed	Growth rate ($\mu\text{m}^2 \text{s}^{-1}$)	Hyphal diameter (μm)	Spk diameter (μm)	Ratios		
					Growth rate/hyphal diameter	Growth rate/Spk diameter	Hyphal diameter/Spk diameter
Wild-type	19	1.40 ^a	9.94 ^a	1.37 ^a	0.13	1.01	7.66
<i>ro-1</i>	24	0.63 ^b	7.21 ^b	0.87 ^b	0.09	0.87	9.02
<i>ro-3</i>	20	0.50 ^b	6.54 ^b	0.83 ^b	0.07	0.65	8.17

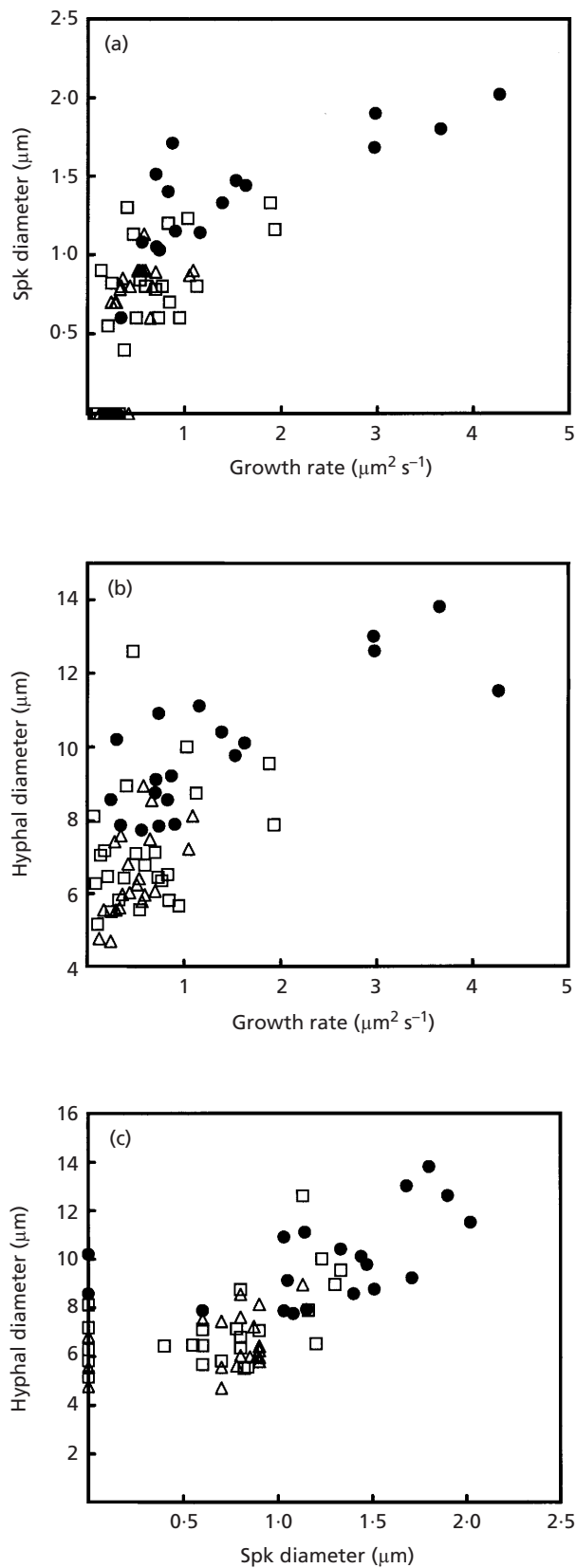


Fig. 4. Correlation between growth rate, hyphal diameter and Spk diameter in hyphae of *N. crassa* wild-type (●), *ro-1* (□) and *ro-3* (△).

Growth rate and Spk size

Hyphal elongation is traditionally used as a measurement of the growth rate. This method is accurate provided the hypha maintains a relatively constant shape during elongation. For the *ropy* mutants, with their distorted hyphal morphology, this method was clearly not valid. Instead, we measured growth rate as increase in cell area per unit of time (Table 2) and calculated that the mean growth rate of hyphae of *ro-1* and *ro-3* was 45 and 34%, respectively, of that in wild-type hyphae. There was no significant difference in growth rate between the two *ropy* mutants (Table 2).

Growth rate was correlated with the presence and size of the Spk in hyphae of both wild-type and the *ropy* mutants (Table 1; Fig. 4a). In general, faster-growing hyphae exhibited a larger Spk; this was true for both the wild-type and the mutants. A large well-defined Spk was the rule in wild-type hyphae (Figs 3a, b); only a few hyphae with growth rates lower than $0.35 \mu\text{m}^2 \text{s}^{-1}$ (i.e. <10% the rate of the fastest-growing hyphae) failed to exhibit a Spk (Fig. 3c). In the two *ropy* mutants, even the fastest-growing hyphae tended to show a Spk that was less phase-dark and smaller than the wild-type (Fig. 3d, e, g, h). Slow-growing hyphae showed only a very small Spk and none was observed in the slowest hyphae. On average, the Spk diameter of *ro-1* and *ro-3* was 62% and 60%, respectively, of that in wild-type (Table 2). Expressed as cross-sectional area, the relative size of the Spk of *ro-1* and *ro-3* becomes 46% and 41%, respectively, of the wild-type Spk, values that approximate the comparative growth rates calculated above.

Hyphal growth rate and Spk size were further correlated with hyphal diameter in both wild-type and *ropy* mutants (Tables 1 and 2, Fig. 4b, c). In *ro-1* and *ro-3* hyphae, hyphal diameter was difficult to assess because of the irregularities of the hyphal shape. Therefore, we estimated mean diameters by dividing hyphal area by hyphal length. In the wild-type hyphae, there was a positive correlation between growth rate and hyphal diameter. The faster-growing hyphae, which had a large Spk, had the largest diameter (Table 1, Fig. 4b). In the mutants, the same tendency could be observed (Table 1, Fig. 4b).

The appearance and size of the Spk varied greatly during growth, particularly in the *ropy* mutants. For instance, during the observation of a hyphal tip of *N. crassa ro-1* growing at $0.6\text{--}0.7 \mu\text{m}^2 \text{s}^{-1}$, a smaller and less phase-dark Spk was visible for about 220 s (Fig. 5), then the Spk disappeared, coinciding with a sharp decrease of the growth rate to $0.1 \mu\text{m}^2 \text{s}^{-1}$. When the growth rate returned to almost the original values ($0.5 \mu\text{m}^2 \text{s}^{-1}$), the Spk became visible again.

Spk trajectory

The Spk of wild-type hyphae of *N. crassa* follows an intricate trajectory produced by a dominant forward motion accompanied by frequent, short, transverse

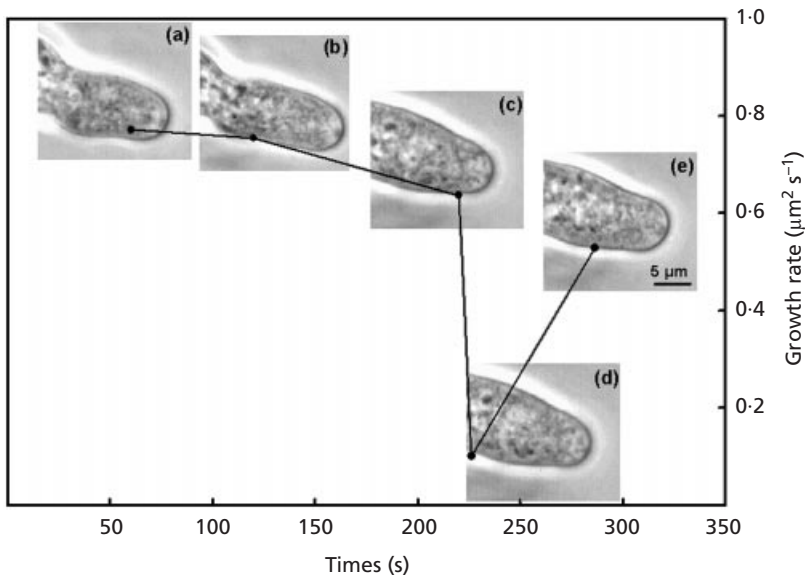


Fig. 5. Growth rate and Spk changes in a hypha of *N. crassa ro-1*. The small Spk observed from (a) to (c) is no longer visible in (d), coinciding with a drastic decrease of the growth rate. As growth rate recovers, a small Spk starts being visible again (e).

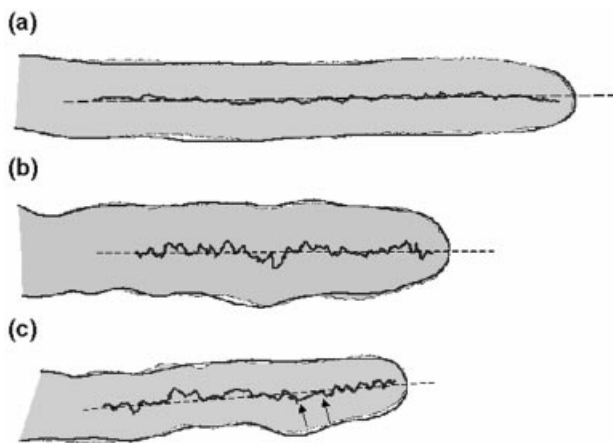


Fig. 6. Computer simulation of hyphal morphogenesis in wild-type and *ropy* mutants. The grey areas are the shapes generated by the Fungus Simulator programmed to follow the Spk paths of (a) wild-type hypha growing for 384 s; (b) *ro-1* hypha growing for 514 s; (c) *ro-3* hypha growing for 491 s. For each hypha, the cell profile (dark solid line) was reconstructed by assembling profiles from three screen displacements. A correction factor was included to compensate for the slight tendency of the microscope stage to drift during the course of the observations (Bracker, 1995). The straight dashed line corresponds to the axis of growth of the cell. Arrows in (c) indicate a data gap in Spk trajectory that occurred during manipulation of the microscope stage. The gap (about 30 s) was filled with a straight line for the simulation. The percentage of mismatch between simulated shape and real shape was 4.5% for wild-type, 4.2% for *ro-1*, and 6.05% for *ro-3*.

oscillations. The trajectory tends to follow the longitudinal cell axis (Fig. 6a). In the distorted hyphae of the *ropy* mutants, the Spk advances with an erratic trajectory that also tends to follow the longitudinal cell axis but with larger and longer-lasting departures (Fig. 6b, c). Minor oscillations in Spk trajectory cancelled each

other and had no apparent impact on the cell profile. However, larger departures in the trajectory of the Spk resulted in corresponding distortions in the morphology of the hypha.

We compared the behaviour of the Spk in *ropy* vs wild-type hyphae by analysing trajectory and growth efficiency. To compare trajectories, we calculated the steadiness index (*S*) (see Methods). In general, the *S* values for wild-type hyphae were higher than those of the *ropy* mutants hyphae (Table 3). In the wild-type, the *S* values were close to 1, indicating a rather steady Spk path, whereas in the *ropy* mutants, the *S* values were considerably lower, indicating a much more erratic movement of the Spk.

To compare Spk efficiency, we assessed the increase in hyphal area per total distance travelled by the Spk and also the rate of Spk advance (total distance per unit time). By both criteria, the *ropy* Spk was less efficient than the wild-type. In area generated per travelled distance, the *ro-1* and *ro-3* Spk were only 71% and 60%, respectively, as efficient as the wild-type Spk (Table 3). In rate of advance, the values were 83% and 72%. These two criteria combined gave overall efficiencies of 59% and 43% compared to wild-type. The latter values correspond to the overall growth rate differences between wild-type and *ropy* mutants (Table 3).

Computer simulation

To analyse the effect of Spk movement on hyphal morphogenesis, the traced Spk trajectories and cell profiles of wild-type and *ropy* mutants were fed to the Fungus Simulator program. The VSC of the simulator was programmed to follow actual Spk trajectories. Cell profiles were used to calculate the amount of vesicles to be released by the VSC at each point in the trajectory. With these two sets of input data, the simulator

Table 3. Spk behaviour and efficiency in three representative hyphae of *N. crassa* wild-type, *ro-1* and *ro-3*

The hyphae analysed are those in Fig. 6.

Strain	Hyphal growth rate			Spk steadiness			Spk efficiency		
	Total increase of area (μm^2)	Time (s)	Growth rate ($\mu\text{m}^2 \text{s}^{-1}$)	Net distance between Spk initial and final position (μm)	Total Spk travelled distance (μm)	Steadiness index (<i>S</i>)	Area/total Spk travelled distance (μm)	Total Spk travelled distance/time ($\mu\text{m s}^{-1}$)	Overall efficiency*
Wild-type	536	384	1.40	53.9	60.4	0.89	8.87	0.16	1.40
<i>ro-1</i>	472	514	0.92	35.0	67	0.52	7.04	0.13	0.92
<i>ro-3</i>	315	491	0.64	33.7	54.7	0.62	5.75	0.11	0.64

* Overall efficiency is the product of (Area/total Spk travelled distance) times (Total Spk travelled distance/time).

duplicated the morphologies of wild-type hyphae and the highly distorted shapes of *ropy* mutants hyphae (Fig. 6).

DISCUSSION

High-resolution video microscopy has allowed us to analyse quantitatively key cellular details of the phenotype of two *ropy* mutants of *N. crassa* (*ro-1* and *ro-3*). We focused this study on the effects of these mutations (dynein and dynactin, respectively), on the behaviour of the Spk and its consequences on hyphal growth and morphogenesis.

Impairment of dynein or dynactin caused major effects at different levels: reduced growth rate, distorted morphology, aberrant cytoplasmic organization, disrupted organelle motility, and a smaller Spk with erratic trajectory. The effects of these mutations on nuclear distribution and mitosis have been previously documented for this and other fungi (Xiang *et al.*, 1994, 1995; Plamann *et al.*, 1994; Tinsley *et al.*, 1996; Bruno *et al.*, 1996; Inoue *et al.*, 1998). Apparently, the reduction in the overall movement of intracellular components along the microtubular cytoskeleton, caused by dynein/dynactin deficiencies, had a general effect on all cytoplasmic activities and hence led to an overall reduction in growth rate. But diminished growth rate need not result in distorted morphology; it should result in slower-growing hyphae with similar morphology. We believe the morphogenetic effects caused by these mutations can be directly ascribed to their impact on Spk formation and behaviour. Invariably, the Spk of *ropy* hyphae was smaller and lacked the stability of the wild-type Spk. The fact that the *ropy* mutants grew poorly and produced deformed hyphae on Petri dish cultures in the dark eliminates the possibility that the Spk deficiencies we observed were caused by stresses imposed on the mutants during microscopy.

Spk size

Presumably, the smaller size of the Spk of *ropy* hyphae is a consequence of a diminished supply of vesicles to the apical region caused by the dynein/dynactin deficiency

in the mutants. This conclusion differs from that made by Seiler *et al.* (1999), who described the *ro-1* mutant as having a ‘prominent’ Spk. However, they apparently did not take into account that the Spk of *ro-1* is considerably smaller than that of the wild-type, and at times may not even be visible, as shown here in Fig. 4 (see also <http://boyce3427.ucr.edu/cytoskel.htm> for video). Consequently, their conclusion that ‘apical transport was intact’ in this *ropy* mutant runs contrary to our evidence, which clearly shows that the processes responsible for Spk formation, including apical vesicle traffic, are affected by dynein deficiency. Inoue *et al.* (1998) also found that dynein is required for normal secretory vesicle transport to the hyphal apex of *Nectria haematococca*.

Since mutations in kinesin are known to affect Spk formation (Seiler *et al.*, 1997; Wu *et al.*, 1998), it was proposed that cytoplasmic microtubules are oriented with their plus ends towards the apex (Lehmler *et al.*, 1997; Seiler *et al.*, 1997, 1999). By the same reasoning, our studies showing that deficiency in cytoplasmic dynein or dynactin affects Spk formation could lead us to the opposite conclusion, namely that the microtubules are oriented with their minus ends towards the apex. Clearly, none of these observations can reveal conclusively the polarity of cytoplasmic microtubules in a hypha. The similarity of phenotypic effects caused by the impairment of opposite motor proteins suggests that both motors are necessary for the maintenance of the Spk and apical growth, but whether or not both are directly involved in the apical transport of secretory vesicles remains to be seen. Possibly, a deficiency in cytoplasmic dynein or kinesin may also impair the endocytotic processes that contribute to the recycling of membranous components from apex to subapex (Hoffmann & Mendgen, 1998), and thus affect Spk formation.

Overall, our analyses showed positive, though not necessarily linear, correlations between Spk size, hyphal growth rate and hyphal diameter in both the wild-type and the *ropy* mutants of *N. crassa*. In general, fast-growing hyphae share a tendency to have a larger hyphal diameter and a larger Spk than slow-growing hyphae.

Similar tendencies were observed in other fungi (López-Franco & Bracker, 1996). Wu *et al.* (1998) found a similar correlation between Spk size, growth rate and hyphal diameter in a kinesin-deletion mutant of *Nectria haematococca*. In other tip-growing cells such as pollen tubes and root hairs, the size of what would be their Spk equivalent (so-called tip body or clear cap) has also been correlated with high growth rate (Reiss & Herth, 1979; Sievers, 1963).

Spk behaviour and morphogenesis

The highly erratic behaviour of the Spk in *ropy* mutants is difficult to interpret since we do not know for sure which cellular components determine the positioning and advance of such a complex and dynamic structure as the Spk. Previously, based on comparative results with benomyl and cytochalasin, we proposed that the microtubule cytoskeleton was directly involved in maintaining the trajectory of the Spk (Riquelme *et al.*, 1998). Our present observations with the dynein-deficient *ropy* mutants lend support to the notion that the microtubule cytoskeleton plays a major role in the formation and behaviour of the Spk. Similarly, Wu *et al.* (1998) showed that kinesin was essential for normal positioning of the Spk in hyphae of *N. haematococca*. All this leads us to conclude that microtubule-associated motor proteins are necessary for maintenance of a high growth rate, a rather steady Spk and a near-perfect hyphoid shape.

Regardless of the exact mechanism controlling the position of the Spk, we have reason to conclude that the erratic trajectory of the Spk is directly responsible for the distorted morphology of *ropy* hyphae. As we did in studying other morphogenetic processes (Bartnicki-García *et al.*, 1995; Reynaga-Peña & Bartnicki-García, 1997; Riquelme *et al.*, 1998), we used the Fungus Simulator to test the correlation between Spk trajectory and cell shape. The simulator generated forms that reproduced the distorted morphology of the *ropy* hyphae. This indicates that the fungal Spk, operating as a VSC, is the structure that ultimately controls the shape of fungal hyphae. In wild-type hyphae, the Spk advances in a fixed direction with only minor transverse oscillations. The spatially uniform vesicle traffic emanating from such a Spk produces a smooth regular shape that approximates the ideal 'hyphoid' shape stipulated by the hyphoid equation (Bartnicki-García *et al.*, 1989). In the *ropy* hyphae, sustained departures in the trajectory of the Spk result in corresponding distortions in the morphology of the hypha.

Barring pleiotropic effects caused by the *ropy* mutations, the dynein/dynactin deficiency probably causes morphogenetic effects by (1) diminishing the traffic of secretory vesicles from their synthesis site (endoplasmic reticulum) either to intermediate secretory compartments or to the hyphal apex; (2) affecting the organization and movement of the growing microtubules; and/or (3) impeding the proper recycling of material needed for normal apical growth to proceed.

ACKNOWLEDGEMENTS

We would like to thank Dr Stuart Brody from the University of California, San Diego, and Dr Leah Haimo from the University of California, Riverside, for helpful suggestions during the course of this work. Ms Riquelme was supported by a Research Assistantship from the University of California, Riverside.

REFERENCES

- Bartnicki, D. D., Gierz, G. & Bartnicki-García, S. (1994). "Fungus Simulator": a Windows application to model fungal morphogenesis. In *Abstracts of the 5th International Mycological Congress, Vancouver, Canada*, p. 12.
- Bartnicki-García, S. (1968). Cell wall chemistry, morphogenesis, and taxonomy of fungi. *Annu Rev Microbiol* **22**, 87–107.
- Bartnicki-García, S. (1973). Fundamental aspects of hyphal morphogenesis. In *Microbial Differentiation*, pp. 245–267. Edited by J. M. Ashworth & J. E. Smith. Cambridge: Cambridge University Press.
- Bartnicki-García, S. & Lippman, E. (1969). Fungal morphogenesis. Cell wall construction in *Mucor rouxii*. *Science* **165**, 302–304.
- Bartnicki-García, S., Hergert, F. & Gierz, G. (1989). Computer simulation of fungal morphogenesis and the mathematical basis for (hyphal tip) growth. *Protoplasma* **153**, 46–57.
- Bartnicki-García, S., Bartnicki, D. D., Gierz, G., López-Franco, R. & Bracker, C. E. (1995). Evidence that Spitzenkörper behavior determines the shape of a fungal hypha: a test of the hyphoid model. *Exp Mycol* **19**, 153–159.
- Bourett, T. M. & Howard, R. J. (1991). Ultrastructural immunolocalization of actin in a fungus. *Protoplasma* **163**, 199–202.
- Bracker, C. E. (1995). The video-enhanced light microscope: a renaissance tool for quantitative live-cell microscopy. *Zool Stud* **34**, 154–156.
- Bracker, C. E., Murphy, D. J. & López-Franco, R. (1997). Laser microbeam manipulation of cell morphogenesis in growing fungal hyphae. In *Functional Imaging and Optical Manipulation of Living Cells*, pp. 67–80. Edited by D. L. Farkas & B. J. Tromberg. Bellingham, WA: SPIE (International Society for Optical Engineering) (Proceedings of SPIE vol. 2893).
- Bruno, K. S., Tinsley, J. H., Minke, P. F. & Plamann, M. (1996). Genetic interactions among cytoplasmic dynein, dynactin, and nuclear distribution mutants of *Neurospora crassa*. *Proc Natl Acad Sci USA* **93**, 4775–4780.
- Garnjobst, L. & Tatum, E. L. (1967). A survey of new morphological mutants in *Neurospora crassa*. *Genetics* **57**, 579–604.
- Gill, S. R., Schroer, T. A., Szilak, I., Steuer, E. R., Sheetz, M. P. & Cleveland, D. W. (1991). Dynactin, a conserved, ubiquitously expressed component of an activator of vesicle motility mediated by cytoplasmic dynein. *J Cell Biol* **115**, 1639–1650.
- Girbardt, M. (1957). Der Spitzenkörper von *Polystictus versicolor* (L.). *Planta* **50**, 47–59.
- Girbardt, M. (1969). Die Ultrastruktur der Apikalregion von Pilzhypphen. *Protoplasma* **67**, 413–441.
- Gooday, G. W. (1983). The hyphal tip. In *Fungal Differentiation*, pp. 315–356. Edited by J. E. Smith. New York: Marcel Dekker.
- Gow, N. A. R. (1989). Control of the extension of the hyphal apex. *Curr Top Med Mycol* **3**, 109–152.
- Grove, S. N. & Bracker, C. E. (1970). Protoplasmic organization of hyphal tips among fungi. *J Bacteriol* **104**, 989–1009.

- Haimo, L. T. & Thaler, C. D. (1994).** Regulation of organelle transport: lessons from color change in fish. *BioEssays* **16**, 727–733.
- Harold, F. M. (1990).** To shape a cell: an inquiry into the causes of morphogenesis of microorganisms. *Microbiol Rev* **54**, 381–431.
- Hasek, J. & Bartnicki-García, S. (1994).** The arrangement of F-actin and microtubules during germination of *Mucor rouxii* sporangiospores. *Arch Microbiol* **161**, 363–369.
- Heath, I. B. (1994).** The cytoskeleton in hyphal growth, organelle movements, and mitosis. In *The Mycota I: Growth, Differentiation and Sexuality*, pp. 43–65. Edited by J. G. H. Wessels & F. Meinhardt. Berlin & Heidelberg: Springer.
- Hirokawa, N. (1982).** Cross-linker system between neurofilaments, microtubules and membranous organelles in frog axons revealed by the quick-freeze, deep-etching method. *J Cell Biol* **94**, 129–142.
- Hirokawa, N. (1998).** Kinesin and dynein superfamily proteins and the mechanism of organelle transport. *Science* **279**, 519–526.
- Hoch, H. C. & Staples, R. C. (1985).** The microtubule cytoskeleton in hyphae of *Uromyces phaseoli* germlings: its relationship to the region of nucleation and to the F-actin cytoskeleton. *Protoplasma* **124**, 112–122.
- Hoffmann, J. & Mendgen, K. (1998).** Endocytosis and membrane turnover in the germ tube of *Uromyces fabae*. *Fungal Genet Biol* **24**, 77–85.
- Howard, R. J. (1981).** Ultrastructural analysis of hyphal tip cell growth in fungi: Spitzenkörper, cytoskeleton and endomembranes after freeze-substitution. *J Cell Sci* **48**, 89–103.
- Howard, R. & Aist, J. R. (1977).** Effects of MBC on hyphal tip organization, growth, and mitosis of *Fusarium acuminatum*, and their antagonism by D₂O. *Protoplasma* **92**, 195–210.
- Howard, R. J. & Aist, J. R. (1980).** Cytoplasmic microtubules and fungal morphogenesis: ultrastructural effects of methyl benzimidazole-2-ylcarbamate determined by freeze-substitution of hyphal tip cells. *J Cell Biol* **87**, 55–64.
- Inoue, S., Turgeon, B. G., Yoder, O. C. & Aist, J. R. (1998).** Role of fungal dynein in hyphal growth, microtubule organization, spindle pole body motility and nuclear migration. *J Cell Sci* **111**, 1555–1566.
- Lehmle, C., Steinberg, G., Snetselaar, K. M., Schliwa, M., Kahmann, R. & Böölker, M. (1997).** Identification of a motor protein required for filamentous growth in *Ustilago maydis*. *EMBO J* **16**, 3464–3473.
- López-Franco, R. (1992).** *Organization and dynamics of the Spitzenkörper in growing hyphal tips*. PhD dissertation, Purdue University, West Lafayette, IN.
- López-Franco, R. & Bracker, C. E. (1996).** Diversity and dynamics of the Spitzenkörper in growing hyphal tips of higher fungi. *Protoplasma* **195**, 90–111.
- McClure, W. K., Park, D. & Robinson, P. M. (1968).** Apical organization in the somatic hyphae of fungi. *J Gen Microbiol* **50**, 177–182.
- McKerracher, L. J. & Heath, I. B. (1987).** Cytoplasmic migration and intracellular organelle movements during tip growth of fungal hyphae. *Exp Mycol* **11**, 79–100.
- Marsden, J. E., Tromba, A. J. & Weinstein, A. (1993).** *Basic Multivariable Calculus*. New York: Springer.
- Paschal, B. M., Shpetner, H. S. & Vallee, R. B. (1987).** MAP 1C is a microtubule-activated ATPase which translocates microtubules in vitro and has dynein-like properties. *J Cell Biol* **105**, 1273–1282.
- Plamann, M., Minke, P. F., Tinsley, J. H. & Bruno, K. S. (1994).** Cytoplasmic dynein and actin-related protein Arp1 are required for normal nuclear distribution in filamentous fungi. *J Cell Biol* **127**, 139–149.
- Reiss, H. D. & Herth, W. (1979).** Calcium gradients in tip growing plant cells visualized by chlorotetracycline fluorescence. *Planta* **146**, 615–621.
- Reynaga-Peña, C. G. & Bartnicki-García, S. (1997).** Apical branching in a temperature sensitive mutant of *Aspergillus niger*. *Fungal Genet Biol* **22**, 153–167.
- Riquelme, M., Reynaga-Peña, C. G., Gierz, G. & Bartnicki-García, S. (1998).** What determines growth direction in fungal hyphae? *Fungal Genet Biol* **24**, 101–109.
- Roberson, R. W. & Vargas, M. M. (1994).** The tubulin cytoskeleton and its sites of nucleation in hyphal tips of *Allomyces macrogynus*. *Protoplasma* **182**, 19–31.
- Schroer, T. A. & Sheetz, M. P. (1991).** Two activators of microtubule-based vesicle transport. *J Cell Biol* **115**, 1309–1318.
- Seiler, S., Nargang, F. E., Steinberg, G. & Schliwa, M. (1997).** Kinesin is essential for cell morphogenesis and polarized secretion in *Neurospora crassa*. *EMBO J* **16**, 3025–3034.
- Seiler, S., Plamann, M. & Schliwa, M. (1999).** Kinesin and dynein mutants provide novel insights into the roles of vesicle traffic during cell morphogenesis in *Neurospora*. *Curr Biol* **9**, 779–785.
- Sievers, A. (1963).** Beteiligung des Golgi-Apparates bei der Bildung der Zellwand von Wurzelhaaren. *Protoplasma* **56**, 188–192.
- Steinberg, G. & Schliwa, M. (1996).** Characterization of the biophysical and motility properties of kinesin from the fungus *Neurospora crassa*. *J Biol Chem* **271**, 7516–7521.
- Tinsley, J. H., Minke, P. F., Bruno, K. S. & Plamann, M. (1996).** p150^{Glued}, the largest subunit of the dynactin complex, is nonessential in *Neurospora* but required for nuclear distribution. *Mol Biol Cell* **7**, 731–742.
- Trinci, A. P. J. (1978).** Wall and hyphal growth. *Sci Prog* **65**, 75–79.
- Turian, G. (1978).** The “Spitzenkörper”, centre of the reducing power in the growing hyphal apices of two septomycetous fungi. *Experientia* **34**, 1277–1279.
- Vale, R. D., Reese, T. S. & Sheetz, M. P. (1985).** Identification of a novel force-generating protein, kinesin, involved in microtubule-based motility. *Cell* **42**, 39–50.
- Vierula, P. J. (1996).** The genetics of morphogenesis in *Neurospora crassa*. In *Patterns in Fungal Development*, pp. 87–104. Edited by S.-W. Chiu & D. Moore. Cambridge: Cambridge University Press.
- Vogel, H. J. (1956).** A convenient growth medium for *Neurospora* (Medium N). *Microb Genet Bull* **13**, 42–43.
- Wu, Q., Sandrock, T. M., Turgeon, B. G., Yoder, O. C., Wirsal, S. G. & Aist, J. R. (1998).** A fungal kinesin required for organelle motility, hyphal growth, and morphogenesis. *Mol Biol Cell* **9**, 89–101.
- Xiang, X., Beckwith, S. M. & Morris, N. R. (1994).** Cytoplasmic dynein is involved in nuclear migration in *Aspergillus nidulans*. *Proc Natl Acad Science USA* **91**, 2100–2104.
- Xiang, X., Roghi, C. & Morris, N. R. (1995).** Characterization and localization of the cytoplasmic dynein heavy chain in *Aspergillus nidulans*. *Proc Natl Acad Sci USA* **92**, 9890–9894.

Received 5 January 2000; revised 29 March 2000; accepted 25 April 2000.